Local structures and interface morphology of $In_xGa_{1-x}As_{1-y}N_y$ thin films grown on GaAs

Y. L. Soo, S. Huang, and Y. H. Kao
Department of Physics, State University of New York at Buffalo, Amherst, New York 14260

J. G. Chen
Department of Materials Science and Engineering, University of Delaware, Newark, Delaware 19716

S. L. Hulbert
Brookhaven National Laboratory, Upton, New York 11973

J. F. Geisz, Sarah Kurtz, and J. M. Olson
National Renewable Energy Laboratory, 1617 Cole Boulevard, Golden, Colorado 80401

Steven R. Kurtz, E. D. Jones, and A. A. Allerman
Sandia National Laboratory, Albuquerque, New Mexico 87185
(Received 4 February 1999; revised manuscript received 26 May 1999)

X-ray absorption fine-structure techniques have been utilized to probe the short-range structures around N and In in $In_xGa_{1-x}As_{1-y}N_y$ compounds containing about 3% of N and 8% of In. Our results indicate that N impurities most likely substitute for As atoms in the system. The In-As interatomic distance in these compounds remains practically the same as in InAs, while the coordination number of As atoms around In shows possible variations with changes in the material characteristics. The N atoms play an important role in affecting the changes of band gap while also serving as ''strain moderators'' by providing a tensile strain in the film to counteract the compressive strain caused by the In impurities. Further, grazing incidence x-ray scattering measurements of $In_xGa_{1-x}As_{1-y}N_y$/GaAs heterojunctions provide direct evidence that the $In_xGa_{1-x}As_{1-y}N_y$ thin films can indeed be lattice matched to GaAs substrates resulting in a reasonably smooth heterointerface. [S0163-1829(99)11643-6]

I. INTRODUCTION

Multilayer compound semiconductors are most promising contenders for the development of next generation solar cells with expected efficiencies higher than 40%. A plausible first-step improvement of efficiency over the present record-holding $GaInP_2$/GaAs junction device[1] is to add a third semiconductor layer with an energy gap around 1 eV and yet lattice matched to GaAs. The ideal calculated efficiency for this triple-junction system would be 38% for AM0 spectrum, compared to 31% without the third junction.[2] The currently known ''material of choice'' for this goal is a novel quaternary system $In_xGa_{1-x}As_{1-y}N_y$. Previous studies of this system have shown that adding In atoms to GaAs increases the lattice constant and the band gap while incorporating N atoms into GaAs decreases both the lattice constant and the band gap.[3] By an interplay of In and N doping in GaAs, a desirable range of direct band gaps and lattice constants can thus be tailored to suit the needs of advanced photovoltaic applications. For example, the compound $In_xGa_{1-x}As_{1-y}N_y$ can be lattice matched to GaAs with a band gap very close to 1 eV by choosing $x=3y$ with y around 3%. Applications of this compound system in long wavelength laser diodes have already been reported.[3,4]

Although the structure of the $In_xGa_{1-x}As$ system appears to be well explored, the effects of N doping in GaAs are far from clear. The location of N atoms in the host as well as its bonding configuration(s) must be determined at first before other fundamental issues such as the impurity levels, strain effects, and their influence on electron transport can be fully understood. Preparation of $In_xGa_{1-x}As_{1-y}N_y$ compounds with desired physical characteristics (e.g., high-electron mobility) is still a technical challenge at the present time. Moreover, since incorporation of In and N can give rise to compressive and tensile strain in thin films of $In_xGa_{1-x}As_{1-y}N_y$ deposited on GaAs, it is conceivable that the interface morphology at the heterointerface can play an active role in affecting the local structure(s) as well as the mobility or diffusion length of the charge carriers. All these properties are important for photovoltaic applications. Physical studies of the local environment surrounding N and In atoms in this quaternary system and the interface morphology would seem highly desirable.

The x-ray absorption fine structure (XAFS) normally refers to the element-specific short-range structure probing techniques of near-edge x-ray absorption fine structure (NEXAFS) and extended x-ray absorption fine structure (EXAFS). It has been known for some time that core level photoabsorption process can be used to characterize the bonding and structure of systems that do not exhibit long-range order. In the present experiment, we have utilized NEXAFS to determine the local bonding environment about N in $GaAs_{1-y}N_y$ ($y=0.057$) and $In_xGa_{1-x}As_{1-y}N_y$ ($x=0.07-0.08$, $y=0.02-0.03$) compounds. As discussed in several recent reviews,[5] the N K-edge NEXAFS spectrum is directly related to the p-projected density of unoccupied

 ©1999 The American Physical Society

TABLE I. A list of samples studied in the present XAFS experiments.

Sample I. D.	Chemical formula (nominal)	Film thickness (μm)	Band gap (eV)	Experiment
EMC2532	$GaAs_{0.943}N_{0.057}$	1		N *K* NEXAFS
MB023	$In_{0.08}Ga_{0.92}As_{0.97}N_{0.03}$	1	1.03	N *K* NEXAFS
EMC3221	$In_{0.07}Ga_{0.93}As_{0.983}N_{0.017}$	0.6		In *K* EXAFS
PA475	$In_{0.08}Ga_{0.92}As_{0.97}N_{0.03}$	1	1.07	In *K* EXAFS
MB394	$In_{0.08}Ga_{0.92}As_{0.97}N_{0.03}$	1	0.99	In *K* EXAFS
MB395	$In_{0.08}Ga_{0.92}As_{0.97}N_{0.03}$	0.1		In *K* EXAFS

states in nitrides. Based on these observations, the N *K*-edge NEXAFS spectrum can often be used to determine the local electronic and physical structures of nitrogen in various nitride compounds.

Since the dilute In impurities in $In_xGa_{1-x}As_{1-y}N_y$ do not generally form long-range-ordered structures, EXAFS is therefore needed for investigating the *local* structures around In atoms. In the present work, EXAFS measurements were performed at the In *K* edge on four $In_xGa_{1-x}As_{1-y}N_y$ samples with $x=0.07-0.08$, $y=0.02-0.03$. The unique features and detailed description of the EXAFS technique are well known as can be found in several review articles.[6]

In addition to the x-ray absorption spectroscopy studies, experiments of grazing incidence x-ray scattering (GIXS) were also performed on samples of $In_xGa_{1-x}As_{1-y}N_y$ to investigate the interface morphology. This is a nondestructive technique well suited for probing the interfacial roughness and height fluctuations of buried interfaces. Detailed description of this experimental technique and methods of data analysis have been reported elsewhere.[7]

II. EXPERIMENT

$In_xGa_{1-x}As_{1-y}N_y$ and $GaAs_{1-y}N_y$ samples studied in the present experiments were prepared by atmospheric and low-pressure metalorganic vapor phase epitaxy using trimethylgallium, trimethylindium, arsine and 1,1-dimenthylhydrazine. The growth temperatures were between 550° and 650 °C at growth rates of 2.4–7.0 μm per hour. Some characteristics of the samples studied in the present N *K*-edge NEXAFS and In *K*-edge EXAFS experiments are listed in Table I.

The x-ray experiments were performed at National Synchrotron Light Source in Brookhaven National Laboratory. Measurements of N *K*-edge NEXAFS were made at beamline U1A, the In *K*-edge EXAFS and GIXS measurements were carried out at beamline X3B1. For the N *K*-edge NEXAFS spectra, partial electron yield (PEY) from the soft-x-ray irradiated sample was measured as a function of incident-photon energy by using a channeltron detector assembly.[5] A retarding potential of 100 eV was applied in front of the electron detector to repel the low-energy background electrons. Time- and energy-dependent variations of the signal were taken into account by normalizing the PEY data with respect to the incident beam intensity, which was constantly monitored by the electron yield of a fine gold mesh. Another upstream gold mesh coated with nitride was used to provide an energy reference for the NEXAFS measurements. The energy resolution for this experiment was ~0.7 eV near the N *K*-edge region.

Nitrogen *K*-edge NEXAFS spectra obtained from PEY measurements with $GaAs_{0.943}N_{0.057}$ (sample EMC2532) and $In_{0.08}Ga_{0.92}As_{0.97}N_{0.03}$ (sample MB023) compounds are presented in Fig. 1. Since the detailed structural arrangements of the constituent atoms in these compounds are unknown, *ab initio* multiple scattering calculations of the absorption fine structure for the compounds are not reliable for making a direct comparison with these NEXAFS data. Instead, we have taken an empirical approach for a quantitative comparison of these samples with other nitride compounds. Nonlinear curve fitting of these NEXAFS spectra can be achieved by using a combination of linear, arctangent, and Gaussian functions for the intensity of the background, edge-jump, and resonance peaks, respectively, of the following form:

$$I=ax+b+A_0\tan^{-1}\left[\frac{2(x-x_0)}{W_0}\right]+\sum_i\frac{A_i}{W_i}\exp\left[\frac{-4(x_i-x_{c,i})^2}{W_i^2}\right]. \tag{1}$$

Although no precise physical meaning can be associated with Eq. (1), a close fit to the experimental data enables us to determine accurately the centers and widths of the resonance peaks in the spectra, which can then be quantitatively compared with those of known reference compound systems. The resonances in the NEXAFS spectra are interpreted as due to transitions from the bound, localized core levels to quasibound or continuum states. Dipole selection rules allow transitions from the localized $1s$ initial states into p-like empty states. For a comparison of the resonance peaks, the N *K*-edge NEXAFS of a 1.5 μm-thin film of GaN deposited on sapphire was also measured. All the curve fits [solid lines, using Eq. (1)] to the NEXAFS data (circles) of GaN and the two compounds are shown in Fig. 1. The characteristic parameters for the three NEXAFS spectra obtained from this curve fitting are listed in Table II.

Conventional EXAFS measurements around the N *K* edge were also attempted, but without success. The experimental difficulties are mainly caused by the insufficient energy range of soft x-ray that is too short for reliable EXAFS analysis. The measurements are further complicated by ubiquitous oxygen contamination in the samples.

Indium *K*-edge EXAFS measurements were conducted by using a conventional x-ray fluorescence mode detection to probe the local structures around In atoms in

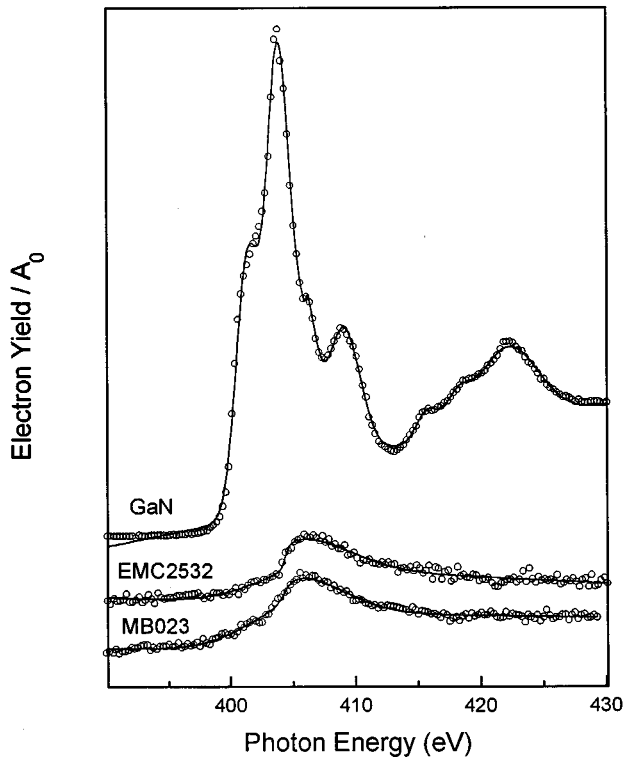

FIG. 1. Nitrogen K-edge NEXAFS spectra. Circles: experimental data; lines: curve-fitting results using Eq. (1).

$In_xGa_{1-x}As_{1-y}N_y$ samples. The experimental setup at beamline X3B1 is similar to that used in our previous EXAFS experiments[8] and all the samples were measured at room temperature. For comparison with a model compound in data analysis, EXAFS spectra of a film consisting of InAs powders were also obtained at the In K edge using transmission mode detection. A well-established background subtraction and correction method was used to extract the EXAFS χ functions from the raw experimental data.[8,9] The χ-functions were then weighted with k and Fourier transformed into real space for detailed analysis.[6] For a quantitative study of the local structures, the experimental data were analyzed and compared with theoretical calculations by a curve-fitting method.[6,8] The EXAFS χ functions and the corresponding Fourier transforms for the four samples studied along with the model compound InAs are shown in Fig. 2. The parameters obtained from this analysis are listed in Table III.

Grazing incidence x-ray scattering (GIXS) experiments on two $In_xGa_{1-x}As_{1-y}N_y$/GaAs heterojunction samples were conducted to investigate the interface morphology of the heterointerface. These two samples (PA474 and PA476) were prepared under the same condition as for PA475 used for the EXAFS study (see Table I). Following the methods described in our previous work,[7] specular reflectivity, longitudinal diffuse scattering (LDS), and transverse diffuse scattering (TDS) scans were made to probe the interfacial roughness and correlations of interface height fluctuations in these samples.

III. RESULTS AND DISCUSSION

Figure 1 shows a comparison of NEXAFS spectra of three nitrides. The spectrum of GaN is very similar to that measured previously by Lambrecht *et al.* from which detailed band-structure correlations with the various N K-edge features[10] have been obtained. The main interest in our present NEXAFS study is to determine whether the local bonding environment about N in $GaAs_{0.943}N_{0.057}$ (sample #EMC2532) and $In_{0.08}Ga_{0.93}As_{0.97}N_{0.03}$ (sample #MB023) is similar to that of GaN and other nitrides. A comparison of the NEXAFS spectra in Fig. 1 and their curve-fitting results in Table II clearly reveal that the peak positions and relative peak intensities of the former two are very different from those of GaN. As demonstrated by Terminello *et al.*[11] for boron nitrides (BN) with various crystal structures, the peak positions of N K-edge features can be used to identify whether N is in sp^2 or sp^3-hybridized configurations. For example, the K-edge feature corresponding to the sp^2-type N generally appears as a relatively sharp peak located between 399 and 402 eV, whereas that for the sp^3-type N is characterized by a broad peak centered around 405 eV. Similar observations have also been reported for transition metal nitrides[5,12] where transitions from the N 1s state to the π^* orbitals (sp^2) and σ^* orbitals (sp^3) typically occur in the NEXAFS spectra at energies below 402 eV and above 405 eV, respectively.

By adopting this empirical correlation, the NEXAFS spectrum of GaN in Fig. 1 indicates that the local bonding environment of N in GaN is in both sp^2 and sp^3-hybridized

TABLE II. Parameters obtained from curve fitting the N K-edge NEXAFS data.

Sample	Edge-jump x_0 (eV)	W_0 (eV)	Peaks x_c (eV)	A/A_0	W (eV)
GaN	406.12	0.19	401.43	45	2.24
			403.89	76	2.17
			405.99	25	2.13
			409.08	32	3.11
			415.71	4	1.92
			418.13	6	2.41
			422.22	35	5.73
$GaAs_{0.943}N_{0.057}$ (EMC2532)	404.35	0.62	405.56	23	9.56
$In_{0.08}Ga_{0.92}As_{0.97}N_{0.03}$ (MB023)	404.24	1.17	405.05	27	9.02

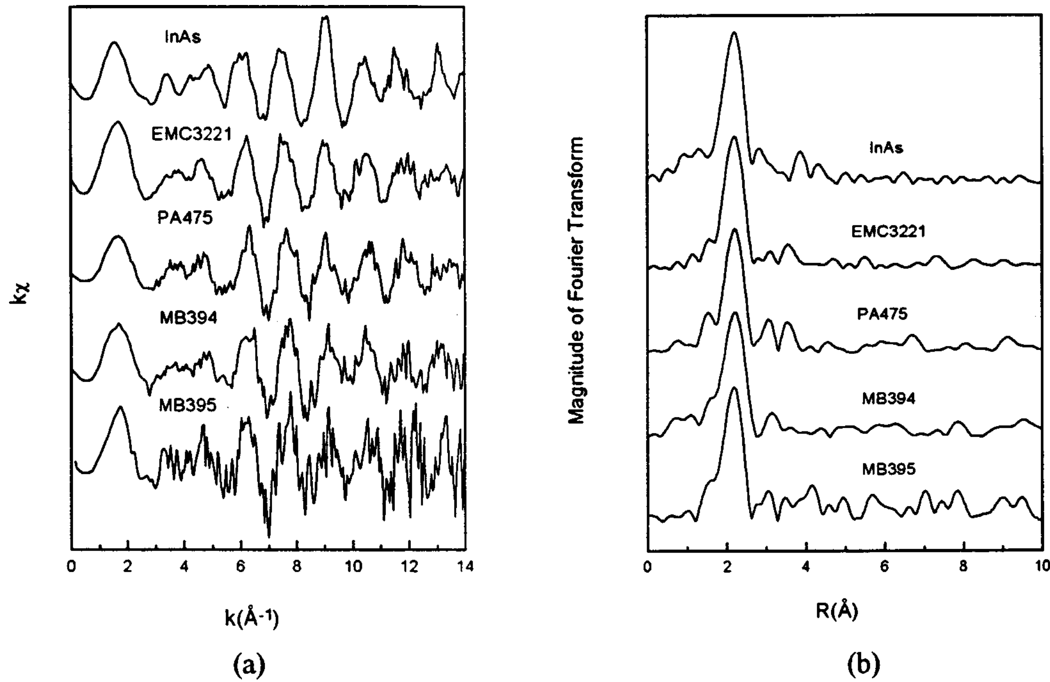

FIG. 2. (a) Weighted In K-edge EXAFS χ functions. (b) Fourier transform of In K-edge EXAFS χ functions shown in (a).

bonding configurations. The detailed nature of this type of bonding configurations of N could be very complicated, the sp^2 character, in addition to showing a strong evidence for transitions from $1s$ to π^* orbitals, might also contain some possible contributions related to extended defects probably present in the material. On the other hand, the N K-edge spectra of $GaAs_{0.943}N_{0.057}$ and $In_{0.08}Ga_{0.92}As_{0.97}N_{0.03}$ are characterized by a *broad* peak centered between 405 and 406 eV, suggesting strongly that nitrogen atoms in these two compounds are in the sp^3-bonding configuration *only*. The NEXAFS results shown in Fig. 1 thus provide the following two conclusions in regard to the local bonding environment of N in these two samples: (i) These two compounds do not consist of physical mixtures of separate GaN and GaAs components, which would have given rise to a N K-edge spectrum including the sharp peaks similar to that of pure GaN. (ii) Considering the tetrahedral (sp^3) configuration about As in bulk GaAs, the observation of sp^3-type nitrogen in these two compounds indicates that the nitrogen atoms most likely substitute for the As atoms in the host.

As for the local environment surrounding the In atoms, we can see from the K-edge EXAFS results in Fig. 2(a) that the k-weighted χ function of the four $In_xGa_{1-x}As_{1-y}N_y$ samples studied is similar to that of the powder InAs model compound. The corresponding Fourier transforms shown in Fig. 2(b) further reveal the resemblance between the In local environment in these $In_xGa_{1-x}As_{1-y}N_y$ compounds and InAs. A prominent peak in the Fourier transform centered at ~2 Å due to the nearest neighbor As shell is present in all the experimental curves. Other possible local structural features beyond this first peak in the Fourier transform are largely contaminated by the background noise, consequently EXAFS data analysis of the higher order neighboring shells becomes unreliable. This result indicates that there is a high degree of local disorder around the In impurities, which masks the possible contributions of higher order neighboring shells to EXAFS in all these $In_xGa_{1-x}As_{1-y}N_y$ samples. The EXAFS data also do not allow enough sensitivity for inves-

TABLE III. Parameters of local structure around In atoms obtained from curve-fitting the In K-edge EXAFS. The EXAFS backscattering amplitude and phase-shift functions are extracted from the data of an InAs model compound with first-shell coordination number (4) and distance (2.6137 Å), obtained from x-ray diffraction data edited by Wyckoff (Ref. 13). N is the coordination number. R is the bond length. $\Delta\sigma^2$ is the difference between the Debye-Waller factors of the samples and the InAs model compound, serving as a measure of local disorder. ΔE_0 is the difference between the zero-kinetic energy value of the sample and that of the model compound. Uncertainties were estimated by using the double-minimum residue ($2\chi^2$) method.

Sample	Atom	N	R (Å)	$\Delta\sigma^2$ (10^{-3} Å^2)	ΔE_0 (eV)
EMC3221	As	4.1 ± 0.2	2.610 ± 0.005	1.2 ± 0.3	2.5 ± 0.5
PA475	As	3.7 ± 0.2	2.601 ± 0.005	1.1 ± 0.3	4.7 ± 0.4
MB394	As	4.3 ± 0.3	2.597 ± 0.005	1.9 ± 0.6	5.1 ± 0.9
MB395	As	5.5 ± 0.5	2.585 ± 0.005	3.7 ± 0.8	1 ± 3

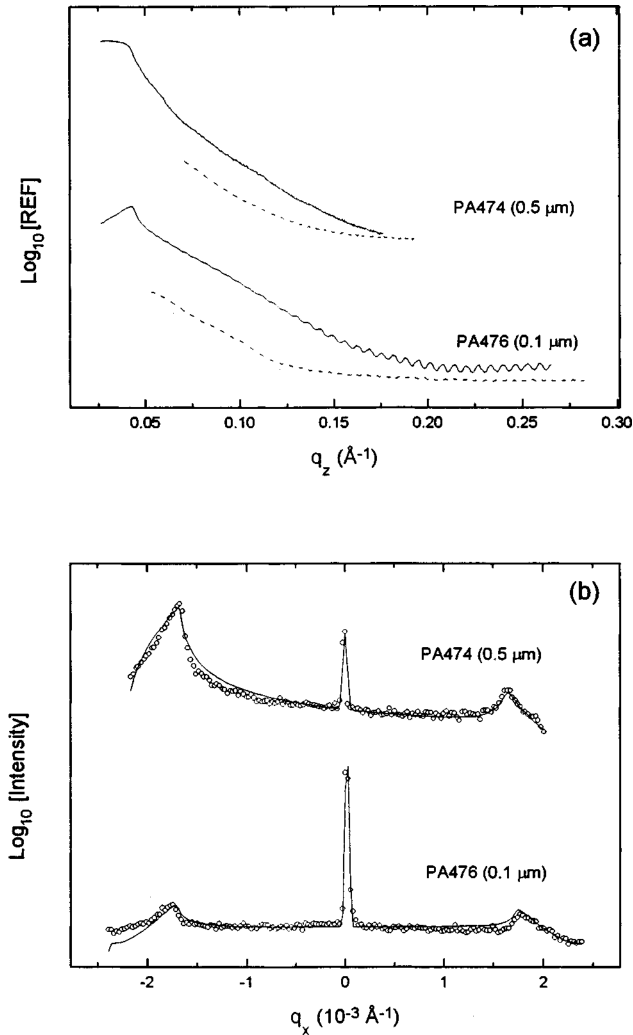

FIG. 3. (a) Specular reflectivity (solid lines) and longitudinal diffuse scattering (dashed lines) data for $In_{0.08}Ga_{0.92}As_{0.97}N_{0.03}$/GaAs heterojunctions. (b) Transverse diffuse scattering results for $In_{0.08}Ga_{0.92}As_{0.97}N_{0.03}$/GaAs heterojunctions. Open circles: experimental data. Solid lines: theoretical calculations.

tigating possible formation of InN in the compound or clustering of the dilute contents of In and N. The final local structure parameters obtained from detailed curve fitting of the first peaks are shown in Table III.

Within the experimental uncertainties of our measurements, the In-As interatomic distance (2.59–2.61 Å) determined for all four $In_xGa_{1-x}As_{1-y}N_y$ samples are practically the same as that in InAs (2.6137 Å) derived from x-ray diffraction data.[13] Although without any further support of local structural information about the higher-order neighboring shells at the present stage, these results are all consistent with the previous EXAFS results obtained with random alloys and epitaxially grown films of $In_xGa_{1-x}As$.[14,15] Hence in these quaternary compounds $In_xGa_{1-x}As_{1-y}N_y$, viewed as a random distribution of low-concentration N impurities ($y\sim1.7-3.0\%$) substituting for As sites in $In_xGa_{1-x}As$, the presence of N atoms does not seem to cause any significant change of the In-As bond length in the $In_xGa_{1-x}As$ host where the dilute ($x\sim7-8\%$) In impurities are also randomly distributed.

On the other hand, the coordination number of first neighbor (As) atoms around the In impurities seems to show some variations with the sample characteristics. As shown in Table III, the As coordination number in sample MB394 (with a band gap of 0.99 eV) is higher than that of sample PA475 (with a 7% larger band gap of 1.07 eV). A thinner sample MB395 (no band-gap data available) which was prepared under exactly the same condition as MB394 shows an even larger As coordination number as well as a higher value of Debye-Waller factor. Although the uncertainties associated with the determination of coordination number are relatively large, a systematic observation of the trend of changes is still possible by a direct comparison of the width and intensity of the Fourier-transform peaks as shown in Fig. 2(b). Samples MB394, MB395, and EMC3221 seem to exhibit a systematically higher coordination number than PA475, all based on a *direct* comparison of the Fourier-transform peak with that of the model compound InAs. An increased local disorder (as suggested by a higher value of Debye-Waller factor) and changes in the As coordination number might be related to the poor charge-carrier mobilities found in these samples. More quantitative understanding of any possible correlation between the coordination number, local disorder, and physical characteristics of materials will require further detailed studies of samples with a wider range variations of composition and processing conditions.

In light of these observations, it can be concluded that N doping in the ternary system $In_xGa_{1-x}As$ not only leads to local structural changes by substituting for the As sites but also could give rise to possible changes in the *local* structure around the In impurities, which in the meantime serves as a strain ''moderator'' by providing a tensile strain to counteract the compressive strain originated from In doping. With the help of about 3% of N substitution, only 8% of In doping is capable of reducing the bandgap of GaAs (1.43 eV) to about 1 eV. On the other hand, if doping by In alone, a large 31% of In is needed (after taking into account the band-gap bowing effect) in order to reduce the band gap of GaAs to 1.0 eV without the help of N doping. Further, the variation of

TABLE IV. Interface parameters obtained from GIXS for $In_xGa_{1-x}As_{1-y}N_y$/GaAS heterojunctions. σ_0, and σ_1 are the rms roughness at the sample surface (air/$In_xGa_{1-x}As_{1-y}N_y$), and rms roughness at $In_xGa_{1-x}As_{1-y}N_y$/GaAs interface, respectively; h is the texture coefficient; $\xi_\parallel$ is the lateral-correlation length.

Sample	$In_xGa_{1-x}As_{1-y}N_y$ (Å)	σ_0 (Å)	σ_1 (Å)	h	$\xi_\parallel$ (Å)
PA476	949±20	10±3	5±3	0.9±0.05	112±23
PA474	4684±60	17±6	14±8	1.0±0.05	116±35

observed band gap at the onset of optical absorption with In and/or N concentrations might actually depend on the *distribution* of these impurity atoms. In the samples studied thus far, the random distribution of both In and N impurities could also give rise to a high degree of local disorder and strain, which could consequently affect the mobilities and diffusion length of the charge carriers. A natural course to follow for improving the photovoltaic characteristics of $In_xGa_{1-x}As_{1-y}N_y$ is therefore to prepare thin films of this compound with more ordered distribution of In and N impurities.

The interface morphology between $In_xGa_{1-x}As_{1-y}N_y$ and GaAs has been examined by using the GIXS technique with two $In_xGa_{1-x}As_{1-y}N_y$/GaAs heterojunctions. Typical results of specular reflectivity, longitudinal diffuse scattering (LDS), and transverse diffuse scattering (TDS) are shown in Fig. 3. The oscillations observed with sample PA476 as shown in Fig. 3(a) indicate a high quality smooth interface. The other sample (PA474) has a larger thickness, hence the oscillations are largely attenuated but still permit a reasonable comparison with the theoretical model. However, the LDS plots of both samples do not show any oscillations, suggesting that there is no correlation between the morphology of the $In_xGa_{1-x}As_{1-y}N_y$/GaAs interface and the top $In_xGa_{1-x}As_{1-y}N_y$ surface in these samples. This result indicates that the presence of microstructural fluctuations in the $In_xGa_{1-x}As_{1-y}N_y$ films could lead to local disorder in the space between successive interfaces, thereby greatly reducing the correlation length in the vertical (film-growth) direction; this observation is also consistent with the absence of higher-order neighbor peaks in the In *K*-edge EXAFS spectra. The TDS results are shown in Fig. 3(b). The data around the central peak and the two side peaks (Yoneda wings) can be fitted very well with theoretical calculations. From a detailed comparison between the data shown in Fig. 3 and theoretical calculations, rms roughness of the top-surface and the interface, the texture coefficient h, and the lateral correlation lengths have been determined. These results are summarized in Table IV. The value of h being close to unity indicates that the distribution of interface height fluctuations in these layer compounds is essentially Gaussian. The interface between $In_xGa_{1-x}As_{1-y}N_y$ and GaAs is quite smooth with a rms roughness generally below 20 Å. On the basis of our previous comparisons of grain sizes determined by AFM and GIXS measurements in various materials, the lateral correlation length values obtained here suggest that the average domain size in these epitaxially grown samples should be about tens of nanometers.

IV. CONCLUSIONS

The compound semiconductor system $In_xGa_{1-x}As_{1-y}N_y$ exhibits many intriguing properties, which are particularly useful for the development of innovative high-efficiency thin film solar cells and long wavelength lasers. The band gap in these semiconductors can be varied by controlling the content of N and In and the thin films can yet be lattice-matched to GaAs. XAFS and GIXS techniques have been employed to probe the local environment surrounding both N and In atoms as well as the interface morphology of several $In_xGa_{1-x}As_{1-y}N_y$ thin films epitaxially grown on GaAs. The results of soft-x-ray XAFS around the nitrogen *K* edge reveal that nitrogen is in the sp^3-hybridized bonding configuration in $GaAs_{1-y}N_y$ ($y=0.057$) and $In_xGa_{1-x}As_{1-y}N_y$ ($x=0.07-0.08$, $y=0.02-0.03$) compounds, suggesting that N impurities most likely substitute for As sites in these two compounds. Within the experimental uncertainties, the results of In *K*-edge XAFS indicate that the In-As interatomic distance remains same as in InAs. The samples studied so far all contain a high degree of local disorder around the In atoms. However, by a direct comparison of the Fourier transforms of the EXAFS signals, a slightly larger coordination number of As nearest neighbors around In atoms was found in a 100 nm-thin film sample of $In_{0.08}Ga_{0.92}As_{0.97}N_{0.03}$. These results show that N substitution of the As sites plays an important role of band-gap-narrowing while in the meantime counteracting the compressive strain caused by In doping. GIXS experiments further confirm that $In_{0.08}Ga_{0.92}As_{0.97}N_{0.03}$ thin films can indeed form very smooth interfaces with GaAs, yielding an average interfacial roughness around 5–20 Å.

ACKNOWLEDGMENTS

We would like to thank Dr. Daniel Friedman for a critical reading of the manuscript and fruitful discussions. The present research at SUNY Buffalo was supported by DOE and NREL.

[1] T. Takamoto, E. Ikeda, H. Kurita, and M. Ohmori, Appl. Phys. Lett. **70**, 381 (1997); K. A. Bertness, S. R. Kurtz, D. J. Friedman, A. E. Kibbler, C. Kramer, and J. M. Olson, *ibid.* **65**, 989 (1994).

[2] S. R. Kurtz, D. Myers, and J. M. Olson, *26th IEEE Photovoltaic Specialists' Conference* (IEEE, New York, 1997), p. 875.

[3] M. Kondow, K. Uomi, A. Niwa, T. Kitatani, S. Watahiki, and Y. Yazawa, Jpn. J. Appl. Phys., Part 1 **35**, 1273 (1996); S. Sato, Y. Osawa, and T. Saitoh, *ibid.* **36**, 2671 (1997).

[4] T. Miyamoto, K. Takeuchi, and F. Koyama, IEEE Photonics Technol. Lett. **9**, 1448 (1997); M. C. Larson, M. Kondow, T. Kitatani, K. Tamura, Y. Yazawa, and M. Okai, *ibid.* **9**, 1549 (1997); M. Kondow *et al.*, Jpn. J. Appl. Phys., Part 1 **35**, 5711 (1996).

[5] J. G. Chen, Surf. Sci. Rep. **30**, 1 (1997), and references cited therein; F. M. F. de Groot, J. Electron Spectrosc. Relat. Phenom. **67**, 529 (1995).

[6] D. E. Sayers and B. A. Bunker, in *X-ray Absorption*, edited by D. C. Koningsberger and R. Prins (Wiley, New York, 1988), p. 211; P. A. Lee, P. H. Citrin, P. Eisenberger, and B. M. Kincaid, Rev. Mod. Phys. **53**, 760 (1981).

[7] Z. H. Ming, A. Krol, Y. L. Soo, Y. H. Kao, J. S. Park, and K. L. Wang, Phys. Rev. B **47**, 16 373 (1993), and references cited therein.

[8] Y. L. Soo, Z. H. Ming, S. W. Huang, Y. H. Kao, R. N. Bhargava, and D. Gallagher, Phys. Rev. B **50**, 7602 (1994).

[9] M. Newville, P. Lïvin, Y. Yacoby, J. J. Rehr, and E. A. Stern, Phys. Rev. B **47**, 14 126 (1993).
[10] W. R. L. Lambrecht, S. N. Rashkeev, B. Segall, K. Lawniczak-Jablonska, T. Suski, E. M. Gullikson, J. H. Underwood, R. C. C. Perea, J. C. Rife, I. Grzegory, S. Porowski, and D. K. Wickenden, Phys. Rev. B **55**, 2612 (1997), and references cited therein.
[11] L. J. Terminello, A. Chaiken, D. A. Lapiano-Smith, G. L. Doll, and T. Sato, J. Vac. Sci. Technol. A **12**, 2462 (1994).
[12] R. Kapoor, S. T. Oyama, B. Fruhberger, and J. G. Chen, Catal. Lett. **34**, 179 (1995).
[13] R. W. G. Wyckoff, *Crystal Structures* (Interscience, New York, 1960).
[14] J. C. Mikkelsen, Jr. and J. B. Boyce, Phys. Rev. B **28**, 7130 (1983).
[15] S. C. Woronick, E. Canova, Y. H. Kao, M. E. Hills, T. W. Nee, and V. Rehn, J. Appl. Phys. **61**, 2836 (1987).